Appl Phys A
DOI 10.1007/s00339-012-6759-z

**Applied Physics A**
**Materials Science & Processing**

# Characterization of excimer laser ablation generated pepsin particles using multi-wavelength photoacoustic instrument

**B. Hopp · G. Kecskeméti · T. Smausz · T. Ajtai · A. Filep · N. Utry · A. Kohut · Z. Bozóki · G. Szabó**

Received: 20 June 2011 / Accepted: 22 December 2011


**Abstract** Preparation of organic thin layers on various special substrates using the pulsed laser deposition (PLD) technique is an important task from the point of view of bioengineering and biosensor technologies. Earlier studies demonstrated that particle ejection starts during the ablating laser pulse resulting in significant shielding effects which can influence the real fluence on the target surface and consequently the efficiency of layer preparation. In this study, we introduce a photoacoustic absorption measurement technique for in-situ characterization of ablated particles during PLD experiments. A KrF excimer laser beam ($\lambda$ = 248 nm, FWHM = 18 ns) was focused onto pepsin targets in a PLD chamber; the applied laser fluences were 440 and 660 mJ/cm$^2$. We determined the wavelength dependence of optical absorption and mass specific absorption coefficient of laser ablation generated pepsin aerosols in the UV–VIS–NIR range. On the basis of our measurements, we calculated the absorbance at the ablating laser wavelength, too. We demonstrated that when the laser ablation generated pepsin aerosols spread through the whole PLD chamber the effect of absorptivity is negligible for the subsequent pulses. However, the interaction of the laser pulse and the just formed particle cloud generated by the same pulse is more significant.

B. Hopp (✉) · Z. Bozóki
Research Group on Laser Physics of the Hungarian Academy of Sciences, Dóm tér 9, 6720 Szeged, Hungary
e-mail: bhopp@physx.u-szeged.hu
Fax: +36-06-62544658

Z. Bozóki
e-mail: zbozoki@physx.u-szeged.hu

G. Kecskeméti · T. Smausz · T. Ajtai · A. Filep · N. Utry · A. Kohut · G. Szabó
Department of Optics and Quantum Electronics, University of Szeged, Dóm tér 9, 6720 Szeged, Hungary

G. Kecskeméti
e-mail: kega@physx.u-szeged.hu

T. Smausz
e-mail: tomi@physx.u-szeged.hu

T. Ajtai
e-mail: ajtai@titan.physx.u-szeged.hu

A. Filep
e-mail: afilep@titan.physx.u-szeged.hu

N. Utry
e-mail: nutry@titan.physx.u-szeged.hu

G. Szabó
e-mail: gszabo@physx.u-szeged.hu

## 1 Introduction

Preparation of different organic thin layers on various special substrates is a quite important task from the point of view of the intensively developing bioengineering and biosensor technologies. The pulsed laser deposition (PLD) technique is a promising procedure for realization of such layers. Previous experiments demonstrated that under appropriate laser parameters the procedure was successfully applied for various biomaterials such as biodegradable polymers [1, 2], enzymes [3–7], proteins [8–10], collagen [11], etc. where the deposited layers retain the biological properties and functionality of the target material.

In spite of these investigations, several open questions remain concerning the material ejection processes during PLD of complex organic molecules. Usually, target pellets are prepared by pressing from powder of the given biomaterial at quite high (several hundred MPa) pressure. According to our earlier developed model, the absorption of laser photons by the particles in the superficial layer of the target results

Published online: 19 January 2012

in chemical and thermal dissociation of the biomolecules within this volume. The fast decomposition gives rise to an explosion-like gas expansion generating recoil forces which tear off and accelerate several solid particles. These ejected grains with sizes from tens of nanometers to a few micrometers containing intact (undamaged) target molecules deposit onto the substrate and form a thin layer. As a consequence, the grown film consists almost exclusively of the intact target biomolecules.

Plausibly, the particle ejection starts within the duration of the ablating laser pulse resulting in significant shadowing effects which can influence the real fluence on the target surface [12–14] and the efficiency of layer preparation. Besides, the produced particle cloud can also absorb the energy of the forthcoming pulses during the deposition process.

Absorption of the ejected grains depends not only on chemical composition but also on their size and morphology [16, 18]; as a consequence, the absorption coefficient measured for the bulk material is not applicable for determination of cloud absorptivity. Therefore, in-situ absorption measurement of ablation generated particle clouds in the PLD chamber is a straightforward way to estimate the shielding effect of the ejected material. Presently, various methods are utilized to measure optical absorption of particles especially in airborne aerosols in their suspended states; however, significant uncertainties are introduced into the absorption determination by those [15–19]. In this study, we introduce a photoacoustic (PA) aerosol absorption measurement technique for in-situ characterization of the ablated particles during PLD experiments. The only instrument that can measure light absorption by aerosols directly is the photoacoustic spectrometer [20], and it was proved to be suitable for in-situ aerosol absorption measurement [21]. Main advantages of this approach are complete insensitivity to scattering particles, filter-free sampling, high sensitivity, and short response time [21, 22].

The measurement is based on the absorption of periodically modulated light followed by non-radiative relaxation of the excited particles leading to a heat transfer of the absorbed energy to the surrounding gas. The subsequent periodic changes of pressure can be detected with a microphone and converted to an electric signal proportional to the mass concentration and also the absorption of the measured analyte. When the light modulation frequency is tuned to an acoustic resonance frequency of a properly designed PA cell, resonant amplification of the PA signal can be achieved. Details of several PA instruments specially designed for airborne aerosol absorption measurement have already been published [21–24]. Most of these instruments operate at a single wavelength in the visible and use the Ångström law to estimate absorption of aerosols in the whole wavelength range. This approach is based on the assumption that the absorbing airborne particles are mainly black carbon (BC) that has a definite wavelength dependence [16, 18]. As compared to BC, other light absorbing carbonaceous or non-carbonaceous particles such as brown carbon ($C_{brown}$), hematite, and bioaerosols (i.e. pepsin) may have significantly different absorption spectra with steeply increasing absorption towards the shorter wavelengths [18]. Therefore, reliability of the deduced absorption far (i.e. in the UV) from the measured wavelengths (i.e. visible) is weak. Our PA instrument (MuWaPas) applied in this study to measure aerosol absorption at four different wavelengths (266, 355, 532, and 1064 nm) was originally developed for airborne aerosol investigation [25]. Moreover, this PA instrument has been proved to be suitable for characterizing absorption features of different types of $C_{brown}$ [26].

The main aim of our experiments was to estimate the effect of the ablation plume on the ablation process itself through the determination of absorption properties of the plume during pulsed laser deposition of biomaterials using our multi-wavelength PA instrument. In the presented investigations, pepsin was applied as model material, because it is an important enzyme having quite complex structure and our earlier studies proved that pepsin thin layers can be fabricated by the PLD method using nano- or femtosecond excimer lasers [2, 3].

## 2 Experiments and results

### 2.1 Experimental arrangement

A KrF excimer laser beam ($\lambda = 248$ nm, FWHM = 18 ns) was focused by a quartz lens ($f = 20$ cm) onto a rotating target placed in the PLD chamber. The targets were pellets pressed from commercially available pepsin powder (FLUKA Chemika) by a Graseby Specac 15011 hydraulic compactor at 245 MPa pressure. The repetition rate of the ablating excimer laser was 1 Hz. The area of the irradiated spot was 0.02 $cm^2$; the applied laser fluences were 440 and 660 $mJ/cm^2$. The aerosols were produced at atmospheric condition and deposited on quartz substrates for scanning electron microscopic (SEM) investigations.

Optical absorption of the laser ablation generated pepsin aerosols was measured by our multi-wavelength photoacoustic instrument applied in the following experimental arrangement (Fig. 1).

The instrument is able to determine optical absorption at four different wavelengths 1064, 532, 355, and 266 nm simultaneously, using the PA detection scheme. The available light powers at these wavelengths are 8 mW at 266 nm, 15 mW at 355 nm, 80 mW at 532 nm, and 360 mW at 1064 nm. The setup of our PA system is described in detail elsewhere [25]. Briefly, the device can be operated in either calibration or measurement mode. In the calibration mode,

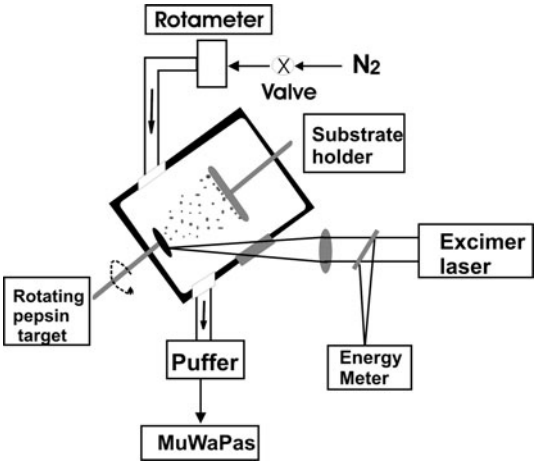


**Fig. 1** Experimental arrangement for characterization of pepsin aerosols produced by excimer laser ablation

the applied four PA cells are illuminated by 532-nm wavelength irradiation while calibration gases with different $NO_2$ concentrations are led through the cells. In the measurement mode, each PA cell is irradiated with one of the four measuring wavelengths simultaneously, and the PA response of the aerosol-loaded gas sample is measured in each cell.

## 2.2 Size distribution

Since spectral behavior of the particles is affected by both their shape and size, at first geometrical parameters such as count median diameter (cmd), shape irregularity, and geometric standard deviation were determined using a scanning electron microscope (Hitachi S4700). A significant part of the ablation generated pepsin aerosols was collected on quartz substrates. Characteristic dimensions of the deposited particles produced by different ablation fluences (440 mJ/cm$^2$ and 660 mJ/cm$^2$) were measured on the basis of the recorded SEM pictures (Fig. 2).

Different size distributions associated with different ablation energies have been found. Pepsin aerosols produced by laser ablation with 440 mJ/cm$^2$ laser energy showed a bimodal size distribution. Thus, we could define two different size regions and calculated the cmd, shape irregularity, and geometric standard deviations of each region independently; the two monodisperse pepsin aerosols had cmd values of 15 nm and 150 nm with geometric standard deviations of 10 and 90 nm. Pepsin aerosols produced at 660 mJ/m$^2$ ablation energy showed one monodisperse size distribution having cmd value of 65 nm with geometrical standard deviation of 30 nm. In both cases, the generated pepsin aerosols showed a nearly compact spherical shape with shape irregularity close to unity.

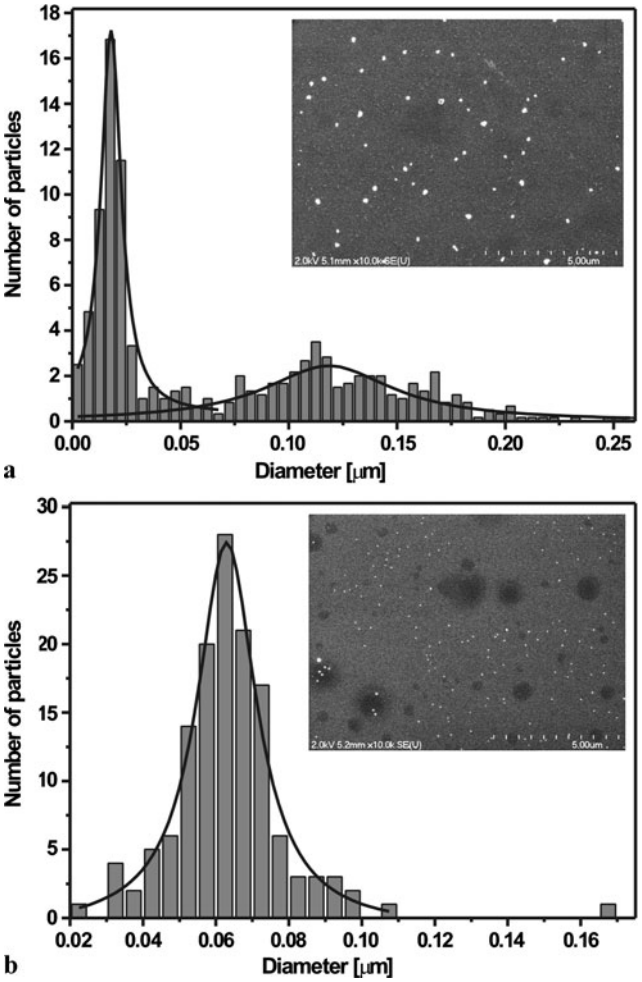


**Fig. 2** Size distributions of deposited pepsin particles at 440 (**a**) and 660 (**b**) mJ/cm$^2$ fluences. Inserted pictures show the recorded SEM images

## 2.3 Determination of wavelength dependence of the mass specific absorption

In our calculation, we used the following equation:

$$S = \sigma_{abs} \cdot \gamma_A \cdot C_{cell} \cdot P_{laser}, \quad (1)$$

where $S$ means the PA signal strength (nV). The mass specific absorption cross section of the analyte ($\sigma_{abs}$) can be determined if the PA setup constant ($C_{cell}$), the laser power ($P_{laser}$, in mW), and the mass concentration of the aerosol-loaded gas sample ($\gamma_A$, in g/m$^3$) are known. $C_{cell}$ represents the PA response generated by unit laser power absorbed by unit optical absorption of the studied molecule (nV/(m$^{-1}$ × mW)). $C_{cell}$ can be determined by calibration with gas standards. The applicability of the gas-phase calibration for aerosol absorption measurement and the calibration procedure are described in detail elsewhere [25]. Briefly, the PA cells of our instrument were calibrated with defined $NO_2$ concentrations at 532-nm wavelength using the

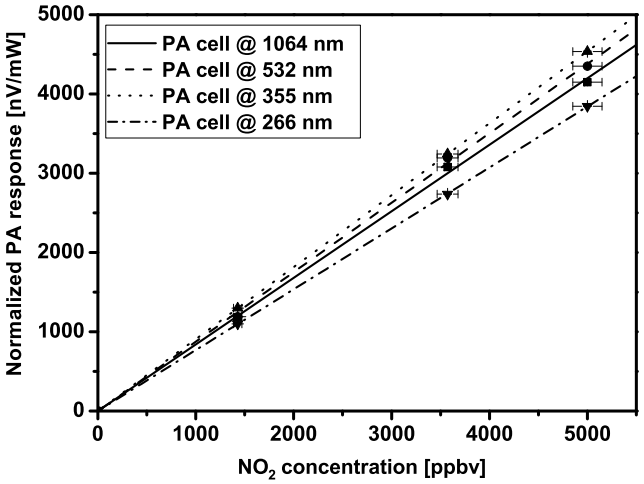


**Fig. 3** The light power normalized PA responses at different $NO_2$ concentrations

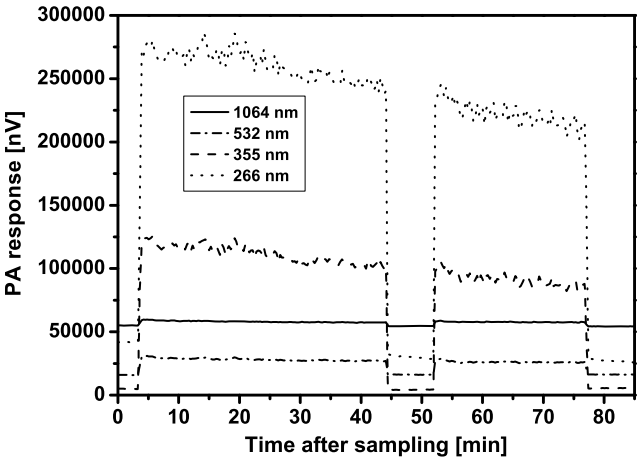


**Fig. 4** PA responses of the generated pepsin aerosols at four different laser wavelengths

**Table 1** Characteristic parameters of the applied PA instrument

| Wavelength [nm] | Cell constant [nV/M $m^{-1}$/mW] | Light power [mW] |
|---|---|---|
| 1064 | 2.29 | 330 |
| 532 | 2.50 | 95 |
| 355 | 2.58 | 18 |
| 266 | 2.17 | 8 |

calibration mode of the instrument in which each cell can be illuminated with 532-nm laser irradiation. Each $C_{\text{cell}}$ was calculated from the slopes of the calibration curves (Fig. 3) on the basis of (2).

$$C_{\text{cell}} = \frac{m}{\alpha^{\text{NO}_2}_{532\text{ nm}} \cdot P_{\text{laser}}} \left[\frac{\text{nV}}{\text{m}^{-1} \cdot \text{mW}}\right], \tag{2}$$

where $m$ is the slope of the calibration curve (nV/ppb), $\alpha$ is the optical absorption of the $NO_2$ gas at 532-nm wavelength ($3.8 \times 10^{-7}$ $m^{-1}$/ppb at 1 atm and 273 K) [27], and $P_{\text{laser}}$ is the laser power at 532-nm wavelength (80 mW). The determined cell constants are summarized in Table 1.

Pepsin pellets were irradiated by the KrF excimer laser to generate pepsin aerosols. The ejected aerosols were suspended in a pure nitrogen gas stream. Nitrogen was used as carrier gas to avoid gas-phase cross sensitivity to ozone at 266 nm. The pepsin aerosols in their suspended state were led into the PA cells for absorption and into the Teflon filter for mass concentration determination by weighing the filter simultaneously. PA signals of each cell were recorded. In order to increase reliability of the measurement, the background (aerosol-free) signal was measured from time to time using a high-efficiently particle (Balston DFU) filter. Results of real-time measurements are shown in Fig. 4. In the first section, the particle-free gas stream was measured, then the particle-containing gas stream was led through the cells and the PA signals at different wavelengths were recorded. In the third section, we measured again the PA strengths of the particle-free gas stream. This measurement cycle was repeated several times. During the whole experiment light powers at the four different wavelengths were also recorded.

The data were evaluated as follows. PA signals measured in both aerosol-free and aerosol-containing gas streams were time averaged. The mean value of the background (BG) signal was subtracted from the mean value of the corresponding PA signal measured in aerosol-containing gas. Taking the BG-corrected PA data and the determined mass concentration value obtained by weighing the aerosols accumulated on the filter, optical absorption and mass specific absorption cross section were derived at the four applied wavelengths according to (1). The measured optical absorptions, $\sigma_{\text{abs}}$, and their wavelength dependences at the investigated fluences are shown in Fig. 5 and summarized in Table 2.

It was found that the laser-generated pepsin aerosols have negligible absorption in the visible and the NIR wavelength regions. The measured curves (solid lines in Fig. 5) were extended down to the 248-nm value (the wavelength of the ablating laser) by fitting an exponential function to the measured values (dotted lines and empty squares).

## 3 Summary and conclusions

In our study, we determined the wavelength dependence of optical absorption and mass specific absorption coefficient of excimer laser generated pepsin aerosols in the UV–VIS–NIR range. Measurement at multiple wavelengths allowed us to extrapolate out of the measured wavelength range as well, for example to calculate these values at the ablating laser wavelength (248 nm).

In the case of pepsin aerosols, we demonstrated that the accuracy of absorption parameters derived from extrapolation on the basis of the measured data depends not only on the number of measuring wavelengths but also on the applied wavelength region (Fig. 5). Generally, the uncertainty of extrapolation is higher in the case of higher Angström exponent (mainly in the UV range); therefore, in this wavelength region it is required to measure absorptions as close to the ablation laser wavelength as possible.

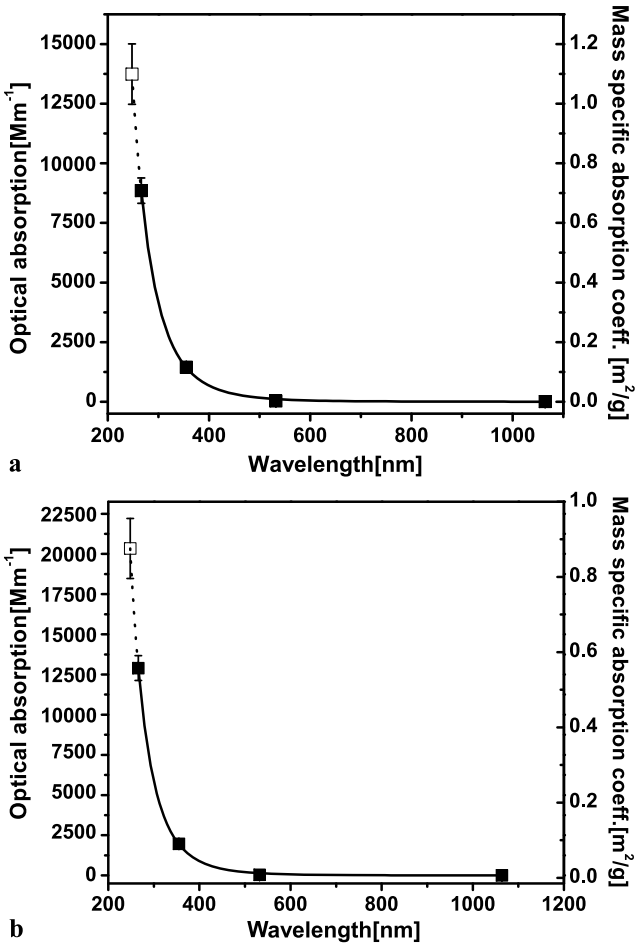


**Fig. 5** Measured (*closed squares*) and fitted (*solid line*) mass specific optical absorption of the pepsin aerosols. The *empty squares* correspond to values calculated on the basis of the line equations. The applied fluences were 440 (**a**) and 660 mJ/cm$^2$ (**b**)

On the basis of absorption measurements and calculations, we could determine the absorbance of the ejected pepsin aerosols in the PLD chamber at the ablating laser wavelength. We distinguished two important cases: (i) a UV pulse ablates the sample resulting in an aerosol cloud spread in the chamber having a dynamic equilibrium and the next pulse enters into this volume, goes through the cloud, and reaches the target surface. (ii) The fore part of an excimer pulse reaches the sample and induces particle ejection generating a relatively dense aerosol cloud which can strongly absorb the further part of the ablating pulse.

Depths of the etched holes was measured at the investigated laser fluences. Knowing the density of pepsin in the pellet, the number of pulses, and the irradiated area, the volume and consequently the mass of the ejected material generated by one UV pulse could be calculated. This was found to be $9.23 \times 10^{-8}$ and $27.01 \times 10^{-8}$ g for 440 and 660 mJ/cm$^2$, respectively. Using these values and the mass specific absorption coefficients, the effect of the aerosol cloud on the real ablating fluence on the sample could be estimated based on the Beer–Lambert law

$$I = I_0 e^{\sigma_{abs} cl}, \tag{3}$$

where $I_0$ is the intensity of the incoming light, $I$ is the remaining intensity after passing through the thickness of the sample, and $c$ is the mass concentration. Taking into account the PLD chamber parameters and the etching geometry, the light path ($l$) and the mass concentration $c$ were calculated in the above-mentioned two cases. Using these values, absolute and relative changes in the intensity of the ablating beam passing through the aerosol cloud could be estimated. These values can be considered as the characteristic parameters for the investigated 'shadowing effect'. Results of these calculations are summarized in Table 3.

According to these data, we made conclusions/estimations on the effect of absorptivity of the ejected pepsin particles on the real fluence on the target surface in the studied cases.

We demonstrated that in the first case where the ablation generated pepsin aerosols spread through the whole chamber having a dynamic equilibrium in concentration (Fig. 6a),

**Table 2** The determined absorption parameters of the investigated pepsin particles at different wavelengths

| Wavelength [nm] | Optical absorption [$\times 10^{-6}$ m$^{-1}$] | | Mass specific absorption coefficient [m$^2$/g] | |
|---|---|---|---|---|
| | 440 mJ/cm$^2$ | 660 mJ/cm$^2$ | 440 mJ/cm$^2$ | 660 mJ/cm$^2$ |
| **1064** | $3.40 \pm 0.07$ | $4.00 \pm 0.08$ | $2.63 \times 10^{-4} \pm 1.5 \times 10^{-5}$ | $1.64 \times 10^{-4} \pm 7.2 \times 10^{-6}$ |
| **532** | $32.05 \pm 1.28$ | $39.28 \pm 1.57$ | $2.48 \times 10^{-3} \pm 1.9 \times 10^{-4}$ | $1.61 \times 10^{-3} \pm 1.0 \times 10^{-4}$ |
| **355** | $1452.24 \pm 87.14$ | $1960.97 \pm 117.66$ | $0.112 \pm 0.011$ | $0.080 \pm 0.007$ |
| **266** | $8853.40 \pm 531.20$ | $12897.09 \pm 773.83$ | $0.685 \pm 0.066$ | $0.528 \pm 0.044$ |
| **248** | **$13742.21 \pm 1264.20$** | **$20341.46 \pm 1871.37$** | **$1.063 \pm 0.18$** | **$0.834 \pm 0.11$** |

**Table 3** Calculated decrease of the ablating fluence on the target surface and the applied parameters taking into account the absorbing effects of the aerosols spread in the PLD chamber (chamber) or forming an aerosol cloud right above the ablated area (plume)

| $F_0$ [mJ/cm$^2$] | 440 | | 660 | |
|---|---|---|---|---|
| | Chamber | Plume | Chamber | Plume |
| $m$ [g] | $9.23 \times 10^{-8}$ | $9.23 \times 10^{-8}$ | $27.01 \times 10^{-8}$ | $27.01 \times 10^{-8}$ |
| $V$ [m$^3$] | $3.14 \times 10^{-4}$ | $4.7 \times 10^{-9}$ | $3.14 \times 10^{-4}$ | $4.7 \times 10^{-9}$ |
| $l$ [m] | 0.11 | 0.0016 | 0.11 | 0.0016 |
| $\sigma_{abs}$ [m$^2$/g] | 1.063 | 1.063 | 0.834 | 0.834 |
| $\Delta F$ [mJ/cm$^2$] | 0.0019 | 13.71 | 0.0067 | 47.42 |
| $\Delta F_{rel}$ [%] | 0.0004 | 3.1 | 0.001 | 7.2 |

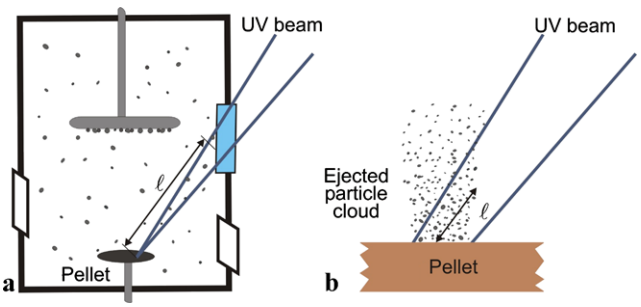


**Fig. 6** Schematic drawings of the two investigated absorption cases

the effect of absorptivity is negligible ($\Delta F_{rel} \ll 1‰$) between the subsequent pulses. However, in the second case, interaction of the laser pulse and the particle cloud generated by the same pulse (Fig. 6b) was more significant; i.e. due to their high concentration, absorptivity of the ejected pepsin particles strongly affected the real fluence reaching the sample during the ablation process. The decrease in the fluence on the target surface can reach several percent depending on the incoming laser fluence. However, this is an overestimation because during our calculation we supposed that the whole ablating laser pulse passes through the ejected particle cloud and the complete ablated volume is transformed into an abundance of particles. The real absorption is lower than the calculated value; however, it is probable that above a certain incoming laser fluence the fluence reduction on the target surface can exceed 10%, which is a significant decrease. It has to be mentioned that this method is applicable in the case of several types of polymers and biomaterials, but it is not valid for highly ionized plasmas and/or metal plumes.

We introduced a photoacoustic measurement technique to measure light absorption of ablation generated aerosols, in situ. The model material was excimer laser ablation generated pepsin aerosol. The interpretation of our experimental results was further supported by the size distribution of the ejected particles on the basis of SEM pictures. We demonstrated that the applied fluences affected the size distribution. It was found that the measured optical absorption increases with increasing ablating fluence, resulting in a higher amount of the ejected material. In contrast with this, the calculated mass specific absorption coefficient decreases with increasing excimer laser fluence. This can be caused by the observed differences in size distribution at the investigated fluences (Fig. 2).

We demonstrated that our multi-wavelength PA instrument is suitable for in-situ spectral characterization of the plume during pepsin ablation in the UV–VIS–NIR wavelength range. In our earlier experiments, it was proved that our system was also able to characterize different types of ablated coal aerosols [26]. On the basis of these studies, we suppose that the presented instrument could be generally applied for characterization of aerosols generated by ablation of other materials, too. The applicability of our procedure is limited by the average dimension of the investigated particles. This limit depends on their chemical composition and the resonance frequency of the applied photoacoustic system. For example, in the case of highly absorbing ($n = 1.75 + 0.75i$) soot particles and 1500 Hz resonance frequency the limiting size is around 3 μm [16].

**Acknowledgements** This work has been supported by the Office for National Research and Technology (NKTH) and the OTKA Foundation from the Hungarian Research and Technology Innovation Fund (project numbers CNK 78549 and K 67818). The authors gratefully acknowledge the financial support of the Hungarian National Office for Research and Technology (JEDLIK_AEROS_EU) and the EUSAAR (European Supersites for Atmospheric Aerosol Research) project.

## References

1. G. Kecskeméti, T. Smausz, N. Kresz, Zs. Tóth, B. Hopp, D. Chrisey, O. Berkesi, Appl. Surf. Sci. **253**, 1185 (2006)
2. B. Hopp, T. Smausz, G. Kecskeméti, A. Klini, Zs. Bor, Appl. Surf. Sci. **253**, 7806 (2007)
3. G. Kecskeméti, N. Kresz, T. Smausz, B. Hopp, A. Nógrádi, Appl. Surf. Sci. **247**, 83 (2005)
4. E. György, F. Sima, I.N. Mihailescu, T. Smausz, B. Hopp, D. Predoi, L.E. Sima, S.M. Petrescu, Mater. Sci. Eng. C **30**, 537 (2010)
5. P.K. Wu, B.R. Ringeisen, J. Callahan, M. Brooks, D.M. Bubb, H.D. Wu, A. Piqué, B. Spargo, R.A. McGill, D.B. Chrisey, Thin Solid Films **398–399**, 607 (2001)

6. T. Xie, A. Wang, L. Huang, H. Li, Z. Chen, Q. Wang, X. Yin, Afr. J. Biotechnol. **8**, 4724 (2009)
7. E. György, A. Pérez Del Pino, G. Sauthier, A. Figueras, J. Appl. Phys. **106**(11), 114702 (2009). doi:10.1063/1.3266670
8. M.A. Hernandez-Perez, C. Garapon, C. Champeaux, Appl. Surf. Sci. **208**, 658 (2003)
9. S. Nagare, J. Sagawa, M. Senna, J. Nanopart. Res. **8**, 37 (2006)
10. Y. Tsuboi, M. Goto, A. Itaya, J. Appl. Phys. **89**, 7917 (2001)
11. Y. Tsuboi, N. Kimoto, M. Kabeshita, J. Photochem. Photobiol. **45**, 209 (2001)
12. S.I. Anisimov, B.S. Luk'yanchuk, A. Luches, Appl. Surf. Sci. **96–98**, 24 (1996)
13. K. Pathak, A. Povitsky, Appl. Surf. Sci. **253**, 6359 (2007)
14. A. Bogaerts, Z. Chen, D. Autrique, Spectrochim. Acta B **63**, 746 (2008)
15. M. Schnaiter, M. Gimmler, I. Llamas, C. Linke, C. Jäger, H. Mutshke, Atmos. Chem. Phys. **6**, 2981 (2006)
16. H. Moosmüller, R.K. Chakrabarty, P.W. Arnott, J. Quant. Spectrosc. Radiat. Transf. **110**, 844 (2009)
17. J. Sandradewi, A.S.H. Prévot, E. Weingartner, R. Schmidhauser, M. Gysel, U. Baltensperger, Atmos. Environ. **42**, 101 (2008)
18. M.O. Andreae, A. Gelencsér, Atmos. Chem. Phys. **6**, 3131 (2006)
19. A. Virkkula, T. Mäkelä, T. Yli-Tuomi, A. Hirsikko, I.K. Koponen, K. Hämerl, R. Hillamo, J. Air Waste Manage. **57**, 1214 (2007)
20. M.O. Andreae, Nature **409**, 671 (2001)
21. D.A. Lack, E.R. Lovejoy, T. Baynard, A. Pettersson, A.R. Ravinshankara, Aerosol Sci. Technol. **40**, 697 (2006)
22. H.A. Beck, R. Niesner, C. Haisch, Anal. Bioanal. Chem. **375**, 1136 (2003)
23. W.P. Arnott, H. Moosmüller, C.F. Rogers, T. Jin, R. Bruch, Atmos. Environ. **33**, 2845 (1999)
24. K. Lewis, W.P. Arnott, H. Moosmüller, C.E. Wold, J. Geophys. Res. **113**, D16203 (2008). doi:10.1029/2007JD009699
25. T. Ajtai, Á. Filep, M. Schnaiter, C. Linke, M. Vragel, Z. Bozóki, G. Szabó, T. Leisner, J. Aerosol Sci. **41**, 1020 (2010)
26. T. Ajtai, Á. Filep, G. Kecskeméti, B. Hopp, Z. Bozóki, G. Szabó, Appl. Phys. A (2010). doi:10.1007/s00339-010-6068-3
27. S. Voight, J. Orphal, J.P. Burrows, J. Photochem. Photobiol. A **149**, 1 (2002)